The Modeling and Observations of Exoplanetary Transits.

Nolan Matthews

May 17, 2013

1 Introduction

In the past 25 years over 861 exoplanetary systems have been discovered and studied using a variety of techniques including radial velocity, transits, gravitational micro-lensing, and even direct imaging (Schneider 2011). The number of confirmed planets continues to grow as more projects and observations are carried out. The number of planets will soon begin to outnumber the amount of scientists studying these objects and the need for more observations will be apparent. The goal of this project was to primarily design an accurate and robust transit curve model (see Fig. 1) and, as a proof of concept, carry out observations at the University of Maryland observatory. The model will possibly be integrated into Brett Morris's OSCAAR photometry code which will allow observers to carry out observations of transits without having to worry about the analysis and model fitting of the data.

With the exception of a few cases, such as the detection of HD 209458b (Charbonneau et al. 2000), using amateur telescopes to discover new exoplanets is a relatively unreasonable expectation. Although detecting new exoplanets may be difficult, follow-up observations of known exoplanets can be both interesting and informative. By adding to the growing database of exoplanetary transits, amateur astronomers are able to make major contributions to the field of exoplanets. Through constraints on the planetary and orbital parameters of an exoplanetary system, the empherdis will be improved aiding in future observations.

Additionally, observations of exoplanets can place constraints on transit times. Variations in transit times over several orbital periods can reveal the interaction of other planets (Holman & Murray 2005, Agol et al. 2005) or even exomoons (Kipping 2009). There should be the ability for amateur astronomers to carry out observations without dealing with the necessary software analysis and model fitting. As the number of exoplanets grow rapidly there will be a need for many follow up observations, which exceeds the amount of profes-

sional telescope time readily available.

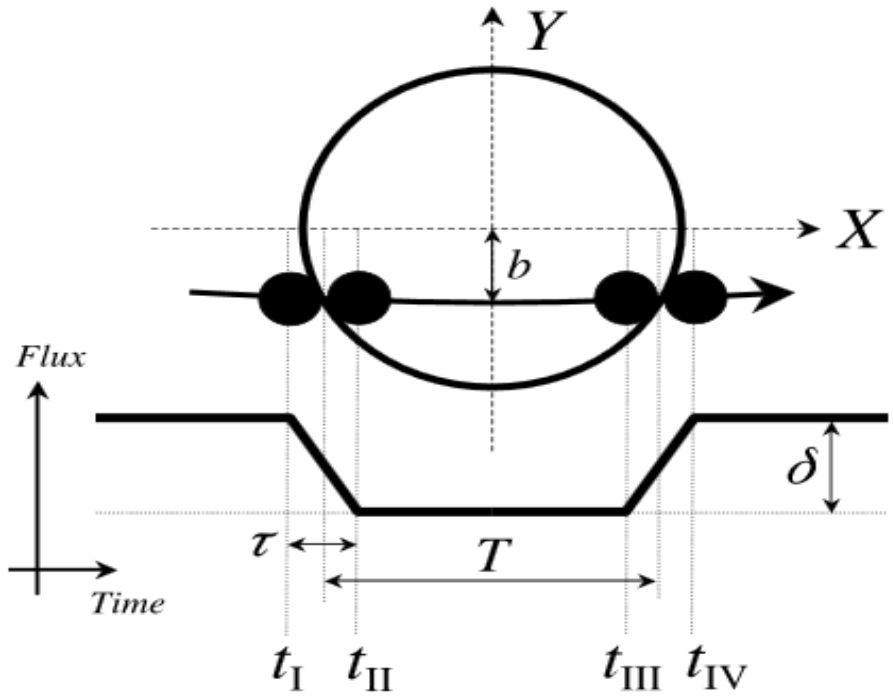

Figure 1: Basic transit geometry for an eclipsing system (Winn 2011). The points of contact are later used to describe orbital and planetary parameters.

The method studied in this paper is exoplantary transits, which occur when the observed exoplanet passes in front of the host star. This situation can only occur when the orbital plane of the planetary system is inclined such that it is edge on. Figure 1 shows the basic schematic for a transiting system. As the planet begins to cross the stellar face, or is in ingress, the observed brightness of the star begins to decrease. The observed flux is at it's minimum value when the planet is half-way through transit. As it begins to leave the stellar face, or is in egress, the observed flux begins to rise quickly until the planet is completely outside the stellar face.

2 Model

During the event of an exoplanetary transit, the light from the host star is eclipsed by the presence of a planet. This is demonstrated by a dip in the observed flux of the host star. The shape of the light curve can reveal a variety of properties describing both the star and orbiting planet. Analytical expressions can be derived (Mandel & Agol, 2002) including the planet/star fractional radius ratio $p = \frac{R_p}{R_{star}}$, the impact parameter b, semi-major axis to star radius ratio $\frac{a}{R_{star}}$.

The model **transiter.py**, uses five different input parameters. Two are the quadratic limb-darkening parameters γ_1 and γ_2 which should generally set to be fixed unless there is precise and accurate data (eg. *Kepler Space Telescope*), since they would be poorly constrained. The limb-darkening parameters can be determined from Claret (2000) and are a function of both stellar properties and observing filter. The model uses four variable parameters, which are as the following:

1. The fractional ratio of the planetary radius to it's host star, $p = \frac{R_p}{R_{star}}$.
2. The impact parameter, b.
3. The velocity of the star across the stellar face $\frac{v}{R_{star}}$.
4. The mid-transit time

Generally, one wants to know the $\frac{a}{R_{star}}$ parameter instead of the orbital velocity. To calculate the scaled stellar radius I use the approximation given in Winn (2009) for a transiting planet,

$$\frac{a}{R_{star}} = \frac{2\delta^{1/4}}{\pi} \frac{P}{\sqrt{{T_{tot}}^2 - {T_{full}}^2}} \frac{(1-e^2)^{\frac{1}{2}}}{1 + e\sin\omega} \tag{1}$$

where δ is the normalized transit depth, T_{tot} is the time difference between first point of ingress and last point of egress, and T_{full} is the time difference between last point of ingress

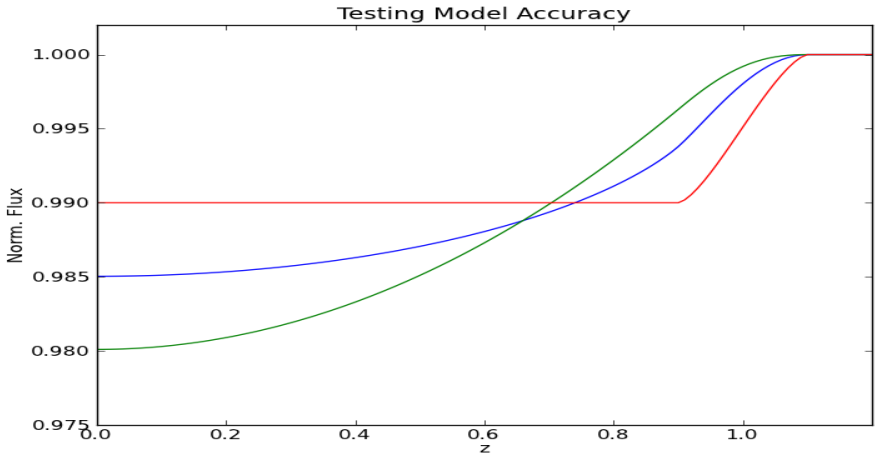

Figure 2: Model output for using $p = 0.1$, $b = 0.0$, with varying limb-darkening parameters. The red line shows output results for $\gamma_1 = 0, \gamma_2 = 0$, blue line has $\gamma_1 = 1, \gamma_2 = 0$, and the green line shows the results for $\gamma_1 = 2, \gamma_2 = -1$

and first point of egress. All of these parameters just mentioned can be deduced directly from the shape of the light curve. In addition to these parameters there are orbital parameters which include the orbital period P, the eccentricity of the orbit e, and the argument of periapsis ω. The orbital parameters cannot be well constrained (if at all) through an observation of a single transit so other methods must be used to measure these values. The period is easily estimated by an observation of more than one transit, whereas ω and the eccentricity are generally constrained through radial velocity measurements (Murray & Correia 2010).

One would also like to know the inclination of the orbit with respect to the observer which can be determined through simple transit geometry,

$$i = \cos^{-1}(\frac{b}{a_{Rstar}}) \tag{2}$$

To make sure that the code was precise I compared it to the data presented in the Mandel & Agol paper for what the curve should look like for a set of fixed parameters as shown in Figure 2. The model output represents represents an extremely similar output as the one

presented in the Mandel & Agol paper. To further test the model's validity it was fitted to a variety of different sets of Kepler data and compared to archival results.

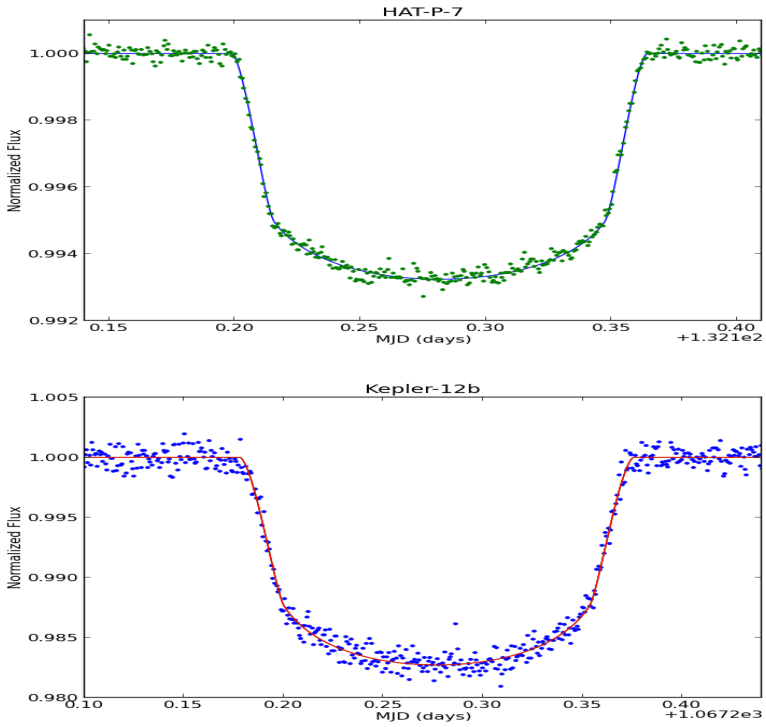

Figure 3: The plots above show different Kepler datasets used to verify the accuracy of the light curve model. The data were taken from the MAST data archive and then were fit to the model. The output parameters are discussed later and are shown in Table 1.

In Tables 1 and 2, we can see that the comparison between the output parameters from the fit using **transiter.py** and archival results are generally in agreement. The parameters compared include the semi-major axis, a, the inclination angle i, and the ratio between the planetary and solar radius, $\frac{R_p}{R_{star}}$ For the Kepler-12b dataset we see that the model parameters are within 1 - 2 σ of the archival results (Fortney et al. 2011). In the case of the HAT-P-7 data, all parameters are within 1- 2 $\sigma$of previous results (A. Pal 2012) with the exception of the semi-major axis.

Table 1: Kepler-12b Model Comparison

		transiter.py	Archival Results
a	AU	0.0554 ± 0.001	0.0556 ± 0.0007
i	^{o}	88.7 ± 1.0	88.76 ± 0.08
$\frac{R_p}{R_{star}}$		0.120 ± 0.001	0.117 ± 0.003

Table 2: HAT-P-7 Model Comparison

		transiter.py	Archival Results
a	AU	0.0347± 0.0001	0.0379± 0.0004
i	^{o}	82.1± 3.0	84.1± 0.2
$\frac{R_p}{R_{star}}$		0.0782± 0.0004	0.079± 0.005

To perform the fit the Levenburg-Marquadt fitting method is performed through the use of the Scipy package, **optimize.curve_fit** where uncertainties are estimated using the square root of the resulting covariance matrix. In most cases it is better to use bootstrapping or prayer bead methods to estimate the uncertainty of a model with several variable parameters. In the case of **transiter.py** this is not entirely feasible as the fitting time is relatively lengthy (2-3 minutes per fit). This issue of speed is discussed later on in the Conclusion section.

For the Kepler data the mid-transit time can be constrained to an uncertainty on the order of tens of seconds. This is an important result as precise measurements are needed to notice any variability in the mid-transit time.

3 Observations and Data Reduction

On the nights of August 18, 2012, October 11, 2012, October 16th, 2012, and April 2, 2013, the planets, respectfully, TrES-1b, Wasp-33b, and Kelt-3 were observed at the University of Maryland observatory in College Park, MD using the 6" and 7" refracting telescopes. They were observed in the z filter, for an exposure length of ranging from about 0.5-2 minutes. The TrES-1b observations were taken by SUMO, a group of fellow undergraduates who perform observations at the University of Maryland observatory. It serves as a great example of the ability for a non-research based observatory to successfully perform observations of transiting exoplanets.

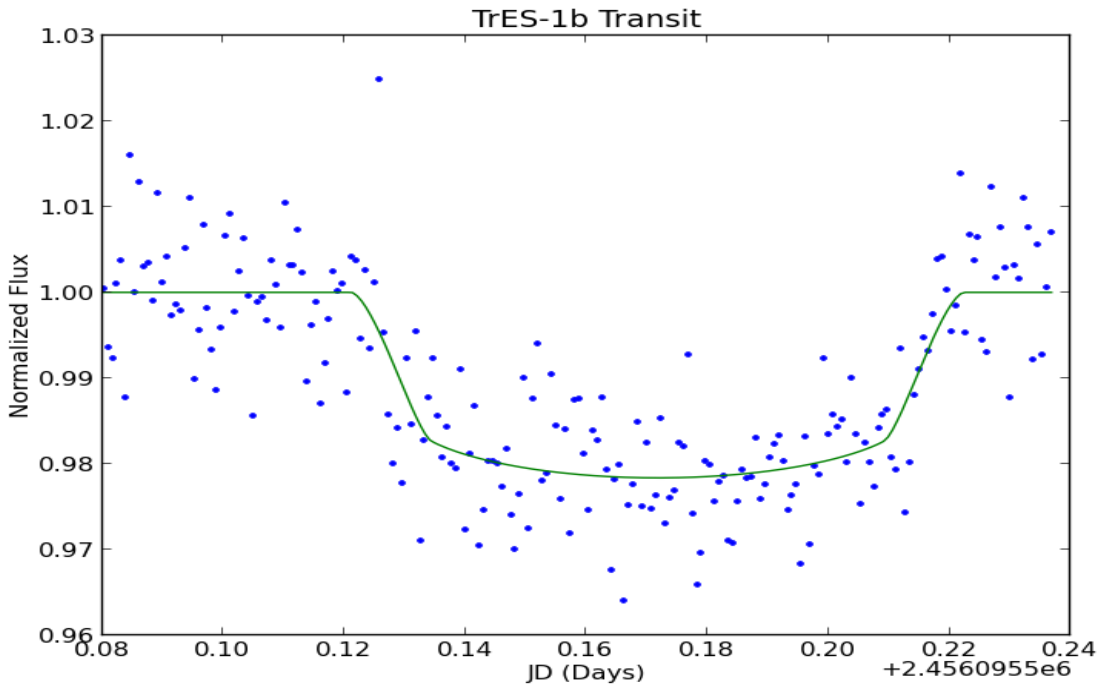

Figure 4: Result for the observation of TrES-1b observed on July 17, 2012. The green line represents the model fit of **transiter.py** where the results are discussed in the text.

Table 3: TrES-1b

		transiter.py	Archival Results
a	AU	0.040 ± 0.007	0.0393 ± 0.007
i	^{o}	88.6 ± 3.4	88.2 ± 1.0
$\frac{R_p}{R_{star}}$		0.138 ± 0.007	0.133 ± 0.009

We see that there is good agreement between the archival data (Southworth 2010) and **transiter.py** model fit. The uncertainties on the parameters is relatively large but, as expected, there is noticeable noise during the transit.

The data for the other observations still need to be reduced. After testing the beta version of OSCAARv2.0 there were numerous bugs which made analysis difficult. When these are sorted out the data sets for the other observations will be processed. If the data sets are high enough quality they will be submitted to the Czech Astronomical Society's transiting exoplanet database to be included in their respective emphermis'.

4 The Flux Time Derivative

In addition to modeling the light curve for a transiting exoplanet, I derived expressions for the flux time derivative for the small planet approximation. The idea was that one could use the time derivative to constrain the mid-transit time. Figure 5 shows a HAT-P-7 light curve along with the numerical time derivative,

As expected, the periods of ingress/egress demonstrate the largest change in flux values. By calculating the time exactly between these maximum and minimum points one can estimate the mid-transit time in a slightly different method. After derivation I found the

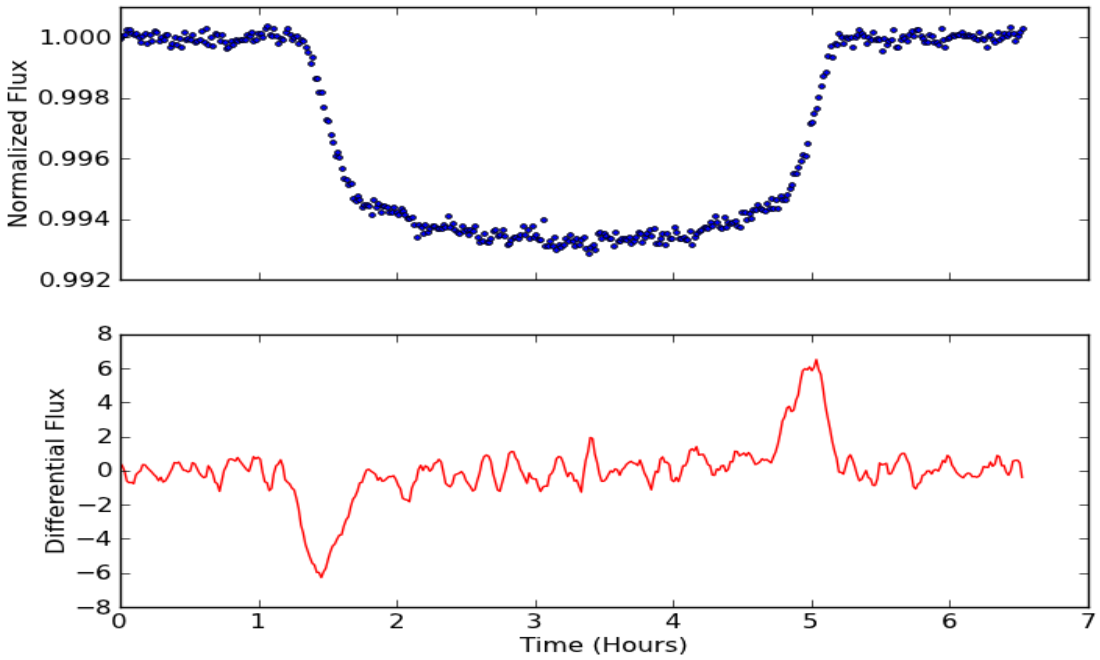

Figure 5: The top panel shows the data from the Kepler Space Telescope of HAT-P-7b. The bottom panel shows the differential flux values of this data set which could be used to calculate the mid-transit time.

differential flux for the small planet approximation (p = $\frac{R}{R_{star}} < 0.1$) to be,

$$\dot{F} = -\frac{1}{4\Omega}[\dot{I}^*(z)\beta + I^*(z)\dot{\beta}] \tag{3}$$

where $\Omega = \frac{1}{4}\left(1 - \frac{\gamma_1}{3} - \frac{\gamma_2}{6}\right)$ for a quadratically limb-darkened star, $a = (z-p)^2$, and $\dot{a} = 2z\dot{z}$. The other variables are as follows,

$$\beta = p^2 cos^{-1}(\frac{z-1}{p}) - (z-1)\sqrt{p^2-(z-1)^2}$$

$$\dot{\beta} = -\dot{z}\left(\frac{p}{\sqrt{1-\left(\frac{z-1}{p}\right)^2}} - \sqrt{p^2-(z-1)^2} + \frac{(z-1)^2}{\sqrt{(p^2-(z-1)^2}}\right)$$

$$I^*(z) = (1-a)\left((1-\gamma_1-\gamma_2) + \frac{2}{3}\sqrt{1-a}(\gamma_1+2\gamma_2) - \frac{\gamma_2}{2}(1-a)\right)$$

$$\dot{I}^*(z) = \dot{a}(1-a)\left[\frac{\gamma_2}{2} + \frac{\gamma_1+\gamma_2}{3\sqrt{1-a}}\right]$$

To make sure that the derived equations are accurate I modeled them using Python software and compared them to a numerical derivative of HAT-P-7 data as shown in Figure 6.

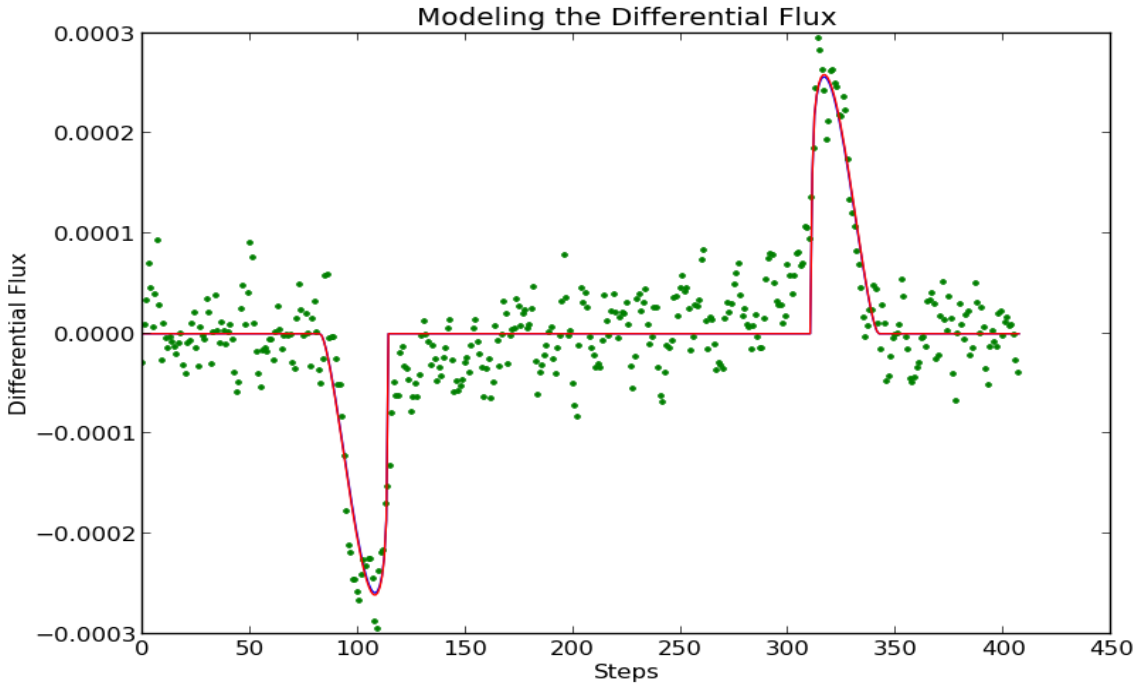

Figure 6: The numerical time derivative of HAT-P-7 data is shown along with the differential flux model for the small-planet approximation. The output parameters are discussed in the text.

It is important to note that the model only covers the case of ingress/egress where the differential flux is the most signficant. The derivation should be extended to model the observed flux between ingress and egress and may account for the descrepancy seen at the those points. Furthermore, the time derivative can also be applied to the case of larger planets but the derivation is relatively lengthy. Equations were derived, but when modeled and applied to data the fit was unable to converge to reasonable output parameters. The output parameters from the fit were close to the values found for the fit from the standard light curve. I found p = 99.5%, $\frac{a}{R_{star}} = 92\%$, and the inclination = 97.5% of the value found above for the normal fit. Error are not presented as the entirety of the light curve should be modeled before stating uncertainties.

5 Conclusion and Future Goals

In this project I have shown that observations of exoplanets can be made without having to deal with the tedious task of data reduction and model fitting. This allows a platform which amateur astronomers can contribute to the exoplanet database by just making observations. In addition it has been shown that observations of transiting exoplanets can be made at even relatively small observatories with generally poor seeing.

The model, **transiter.py** has been shown to be an accurate tool for measuring planetary properties but more gains could be made in some areas. One of the most important things to improve is the speed that the fit is performed. Although Python has proven to be a straightforward programming language it has a significant amount of overhead creating performance issues. There are a variety of ways to approach this topic. The code, currently written in pure python, could be ported to Cython, which uses C extensions for the Python language and has proven to significantly improve performance. Additionally, a relatively new package 'Numba' has been shown to improve Python performance 100 - 1000 times by simply adding

a single line of code to the currently existing script.

The equations describing the flux time derivative of a small-planet approximation were also derived in this project. The flux time derivative could be used to quickly constrain the mid-transit time. Equations for larger planets should be reviewed and investigated to measure the possibility of other parameter constraints.

I would like to gratefully acknowledge the support of my mentor Dr. L. Drake Deming for helpful discussions and guidance on this project. Additionally, Brett Morris and Elizabeth Warner were extremely helpful in learning how to use the observatory equipment and the methods of carrying out observations of exoplanets.

6 Appendix

In Mandel & Agol 2002, they derive analytical expressions which describe the shape of the light curve that account for a variety of orbital and planetary properties. The transit is broken down into a case by case situation where the observed flux are dependent on these properties. Figure 1 below shows a schematic of these different which are further discussed below.

The model **transiter.py** uses the following different cases which uses a quadratically limb-darkened stellar face. The total flux is shown to be,

$$F = 1 - (4\Omega)^{-1}[(1-c_2)\lambda^e + c_2(\lambda^d + \frac{2}{3}\Theta(p-z)) - c_4\eta^d] \tag{4}$$

where $\Omega = \Sigma_{i=o}^{4} c_i(i+4)^{-1}$, $c_1 = c_3 = 0$, $c_2 = \gamma_1 + 2\gamma_2$ $c_4 = -\gamma_2$, $\Theta(p-z)$ is the heavy-side step function. The λ and η parameters are dependent on the specific case of the transit. For case 1, there is no transit and the flux is normalized to be 1. For case 2, the planet is in ingress/egress and the λ/η parameters are,

$$\lambda^e = \frac{1}{\pi}[p^2\kappa_0 + \kappa_1 - \sqrt{\frac{4z^2 - (1+z^2-p^2)^2}{4}}]$$

$$\lambda_d = \lambda_1 = \frac{1}{9\pi\sqrt{pz}}[(1-b)(2b+a-3) - 3q(b-2)K(k) + 4pz(z^2+7p^2-4)E(k) - 3\frac{q}{a}\Pi(\frac{a-1}{a}, k)]$$

$$\eta_d = \eta_1 = (2\pi)^{-1}[\kappa_1 + 2\eta_2\kappa_0 - \frac{1}{4}(1+5p^2+z^2)\sqrt{(1-a)(1-b)}]$$

$$\eta_2 = \frac{p^2}{2}(p^2+2z^2)$$

where $K(k)$ and $E(k)$ are the complete elliptic integrals of the first and second kind, $\Pi(m,k)$ is the complete elliptic integral of the third kind and $k = [(1-a)/(4zp)]^{\frac{1}{2}}$ For the other case when the planet is fully inside the stellar disk, $\lambda^e = p^2$, $\eta^d = \eta_2$

$$\lambda^d = \lambda^2 = \frac{2}{9\pi\sqrt{1-a}}\left[(1-5z^2+p^2+q^2)K * k^{-1} + (1-a)(z^2+7p^2-4)E(k^{-1}) - 3\frac{q}{a}\Pi(\frac{a-b}{a}, k^{-1})\right]$$

References

[1] Holman M. J. and Murray N. W. 2005 Science 307, 1228-1291

[2] Agol E., Steffen J. Sari R. and Clarkson W.. 2005, MNRAS 359, 567-579

[3] Charbonneau, D., Brown, T. M., Latham, D. W., & Mayor, M. 2000, ApJ, 529, L45

[4] Fortney, J. J., Demory, B.-O., Désert, J.-M., et al. 2011, ApJ, 197, 9

[5] Kipping D. M. 2009a MNRAS 392, 181-189

[6] Mandel K., Agol E., 2002, ApJ, 580, L171

[7] Murray, C. D., & Correia, A. C. M. 2011, Exoplanets, edited by S. Seager. Tucson, AZ: University of Arizona Press, 2011, 526 pp. p.15-23, 15

[8] Pal A., Bakos G., Torres G., Noyes R., Fischer D., Johnson J., Henry G., Butler P., Marcy G., Howard A., Sipocz B., Latham D. & Esquerdo G. MNRAS, 401, 2665

[9] Southworth J., 2010, MNRAS, 386, 1644

[10] Winn J. N. et al., 2009, ApJ, 703, 2091